Cross-phase Modulation Wavelength Converter using PLC Hybrid Integration Technologies

Rieko Sato*†, *Toshio Ito, Ikuo Ogawa, and Hiroshi Okamoto

Abstract

We assembled a cross-phase modulation (XPM) wavelength converter by using semiconductor optical amplifier (SOA) and planar lightwave circuit (PLC) hybrid integration technologies. We clarified the optimal current conditions for low input power operation and successfully achieved -10 dBm input signal power operation at 10 Gbit/s without using a signal preamplifier. For stable control of XPM operation, we introduced a novel tuning technique to optimize the input power of the XPM wavelength converter. Using this technique, we could easily set the optimal input power for variable wavelength conversion among 30 wavelengths. We also fabricated an XPM wavelength converter unit containing a variable continuous wave source and confirmed simultaneous and automatic operation.

1. Introduction

All-optical wavelength converters are important components for future photonic networks based on dynamic wavelength path routing [1]. Various types using semiconductor optical amplifiers (SOAs) have been reported. Cross-phase modulation wavelength converters (XPM-WCs) [2]-[5] show high total performance compared with other means of wavelength conversion using SOAs (cross-gain modulation (XGM) and four-wave mixing) in terms of regeneration capability [6], low chirp characteristics on single-mode fiber transmission, noise reduction [7], and so on. As one method of assembling such XPM-WC devices, we have applied hybrid integration technologies [8], [9] on a PLC (planar lightwave circuit) platform. These technologies allow an optical module with at least two I/O (input/output) ports, like an XPM-WC, to be assembled with sufficient reproducibility, and the characteristics of the SOA and PLC can be optimized independently. Moreover, it should be possible to add other functions by inserting a filter or grating and to expand to large-scale-integration circuits by attaching PLCs directly [10].

When such XPM-WCs operate in an optical cross-connect or optical transport system [11], there will be some problems to be solved. One is that the wavelength converter should operate at low optical power so that the system's level diagram can be flexibly designed. For example, a parallel arrangement of XPM-WCs is possible if the required optical power is reduced. In conjunction with this, low power consumption (or low drive current) for the SOA is also needed. In 10-Gbit/s trials reported to date, a relatively high input power of about 0 dBm has always been used. Although an XPM-WC with a monolithically integrated optical preamplifier did achieve 10-Gbit/s operation at input power of -10 dBm, the SOA required a high total current (400–500 mA) [3].

Another issue is a simple control technique for the XPM-WC. It is necessary to adjust two or more tuning parameters (e.g., input signal power, input continuous wave (CW) light power, SOA drive currents, and wavelengths) and operate at the optimal operating point. In addition, these parameters must be readjusted when they are changed. From the practical standpoint, it is important to be able to set the optimal value of these tuning parameters easily. However, there has not been a full report on this before.

This paper describes approaches to optimal operation that addresses the above issues. Using the optimal tuning technique, we develop a control unit that aims to achieve simultaneous operation with a variable CW source.

† NTT Photonics Laboratories
Atsugi-shi, 243-0198 Japan
E-mail: rieko@aecl.ntt.co.jp

2. SOA-PLC hybrid module and approach to optimal tuning

A schematic of an XPM wavelength converter circuit is shown in Fig. 1. It consists of a two-channel SOA (SOA_{mod} and SOA_{pc} for modulation and phase control, respectively) integrated with spot-size converters (SS-SOAs) on a PLC platform. In Figure 1(a), the CW light at a wavelength of λ_c input at port 1 is divided by the 3-dB coupler c1 and sent into the two arms of the interferometer. Then, it is injected into both SOAs, multiplexed by another 3-dB coupler c2, and output at port 2. The signal light at a wavelength of λs is injected into SOA_{mod} through port 3. The input signal light causes a depletion of carrier density in SOA_{mod} and thereby an increase in its refractive index. The relative phase difference of the interferometer $\Delta\phi$ should change from $2n\pi$ to $(2n+1)\pi$ as a result of the change in the refractive index in SOA_{mod}. The phase modulation, caused by the signal input to SOA_{mod}, is converted to an intensity modulation and the converted output signal is output at port 2. The current to SOA_{pc} I_{pc} was set to "inverted-mode" conversion. Figure 1(b) shows an example of the static wavelength conversion curve in "inverted mode", in which the converted output signal power changes in inverse proportion to the input signal power.

The approach to optimal tuning is drawn schematically in Fig. 2. There are four parameters (I_{mod}, I_{pc}, $P_{s\text{-}in}$, and $P_{c\text{-}in}$) to determine the tuning condition. I_{mod} and I_{pc} are the currents to SOA_{mod} and SOA_{pc}, respectively, and $P_{s\text{-}in}$ and $P_{c\text{-}in}$ are the input powers of the signal and CW lights, respectively. For a constant current I_{mod}, we examine the relationships among pairs of the other parameters. As the first approach from the relationship between I_{pc} and $P_{s\text{-}in}$, we clarify the optimal I_{pc} for low optical power operation and find the minimum input signal power at a low total current [12]. As the second approach from the relationship between $P_{s\text{-}in}$ and $P_{c\text{-}in}$, we propose a tuning technique to optimize the two input powers.

Figure 3 shows the structure of a polarization insensitive SS-SOA array [14]. Spot-size converters are butt-coupled to both sides of the 1.55-µm bulk active region of the SOA. The SS-SOA is 1200 µm long (active region: 600 µm, spot-size converter region: 300 µm) and both facets are treated with an antireflection coating. The waveguide is 0.4 µm thick at the butt-joint and 0.2 µm thick at the facet.

A photograph of a hybrid module and a drawing of

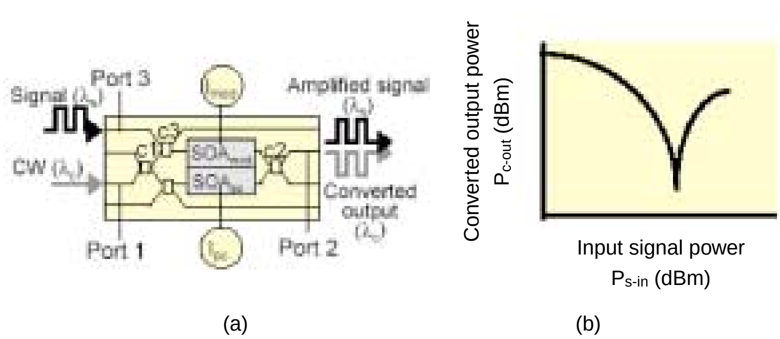

Fig. 1. (a) Schematic of XPM-WC, (b) wavelength conversion curve.

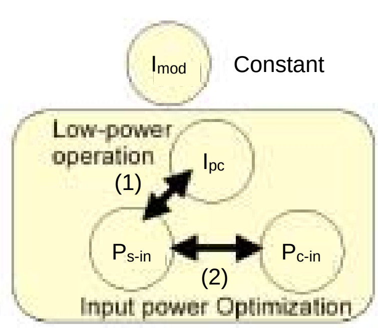

Fig. 2. Approach to XPM optimal tuning.

device assembly are shown in Fig. 4. The SS-SOA array was flip-chip bonded onto the PLC platform, which has a silica-on-silicon structure, using a passive alignment technique [8]. The average coupling loss between the SS-SOA and the PLC waveguide was estimated to be about 4 dB. The total insertion loss from port 1 to the SS-SOA, including the coupling loss between the SS-SOA and the PLC waveguide, was estimated to be about 11 dB. The optical couplers (c1, c2, and c3 in Fig. 2) are multi-mode interference couplers. The PLC waveguide has a refractive index difference of 0.75%. The PLC chip size is $30 \times 3 \times 1$ mm^3. An array of four single-mode fibers was directly attached to each side of the PLC using UV-curable adhesive. A built-in Peltier device in the package precisely controls the module temperature.

3. Low input power and low current operation

Low input power operation is difficult, especially when the drive current of the SOA is low. The reason is as follows. As described in the previous section, there are two currents that have to be controlled in wavelength conversion: I_{mod} and I_{pc}, which work for signal modulation and phase control, respectively. We usually adjust these currents to get the maximum output extinction ratio. But one problem occurs if we make them lower. When I_{mod} is high enough, for example, more than 200 mA, a good output eye pattern is observed. But when it is lowered, the signal degradation becomes strong (Fig. 5(b)). This is due to a consequent increase in the carrier lifetime in the SOA. Under these conditions, since the eye opening will deteriorate, stable low-optical-power operation is difficult.

In order to improve the eye pattern without increasing I_{mod}, we focused on the other SOA current I_{pc}, because the output signal amplitude is controlled by it. To confirm the effectiveness of using I_{pc}, we measured the dependence of the eye opening ratio and the extinction ratio on I_{pc} (Fig. 5(a)) keeping I_{mod} and the input signal power constant. In Fig. 5(a), the left axis shows the eye opening ratio (the ratio between the maximum output amplitude A and the minimum value B) at 10 Gbit/s, and the right axis shows the extinction ratio measured under the static condition. At operating point a shown Fig. 5, where the maximum extinction ratio is obtained, the eye opening ratio is inadequate (Fig. 5(b)). When the extinction ratio decreases as I_{pc} is reduced from operating point a shown Fig. 5, the maximum output amplitude A also decreases. Therefore, the eye opening ratio improves and the maximum value of 0.98 is obtained at operating point b shown Fig. 5. Figure 5(c) shows the improved eye pattern at the optimal operating point b shown Fig. 5, where I_{pc} was reduced to 85 mA.

At the optimal operating point b shown Fig. 5, we examined 10-Gbit/s low power operation. We measured the bit error rate (BER) characteristics for both the input signal (base line) and the converted output signal. The input signal was modulated at 10 Gbit/s (NRZ format, PRBS 2^{31}-1), and its wavelength was 1558.7 nm. The wavelength of CW light was 1535.1

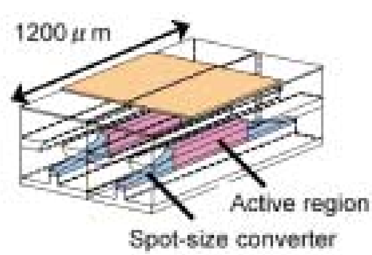

Fig. 3. Structure of SS-SOA array.

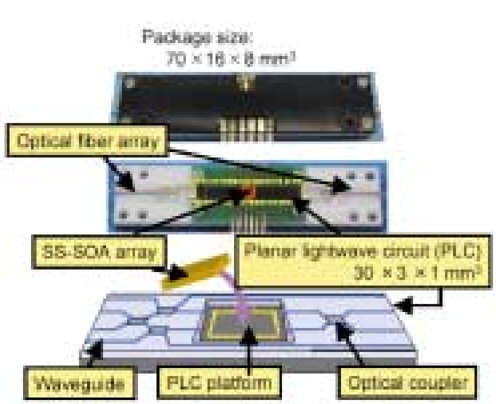

Fig. 4. Hybrid XPM module and device assembly.

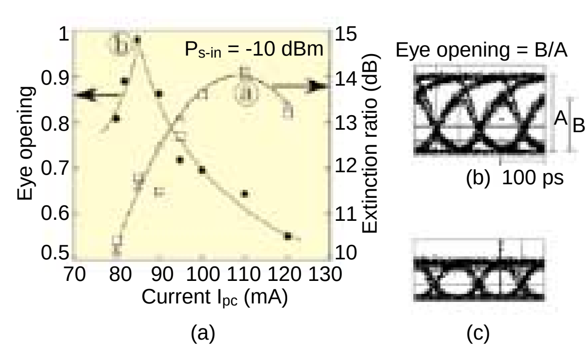

Fig. 5. (a) Dependence of eye opening and extinction ratio on current I_{pc}, (b) eye Pattern at operation point, (c) eye Pattern at operation point.

nm. The input CW power was set to be optimal for each input signal power. Fig. 6 shows the results of BER measurement at input signal power of -10 dBm and its output eye pattern, when I_{pc} was the optimal value (85 mA). The black and white circles show the BER of the input signal and the converted output signal, respectively. The excess power penalty at BER of 10^{-9} was less than 0.5 dB. The power penalty for each input signal power less than -4 dBm is plotted in Fig. 7. The black circles show the value when I_{pc} was optimal (85 mA) and the white circles show the value when I_{pc} was not optimal (110 mA). In the optimal condition, a power penalty of less than 0.5 dB was maintained down to -10 dBm of input signal power, whereas in the unoptimized condition, it was more than 1 dB when the input signal power was lower than -6 dBm. If we take a 1-dB power penalty as a threshold, then the minimum operating input power was improved by at least 4 dB. Moreover, the input CW light power at input signal power of -10 dBm was also -10 dBm, and the SOA total current was reduced to 215 mA. These results indicate that I_{pc} optimization is effective for low-power and low-current operation.

4. Optimal tuning technique and its application to variable XPM-WC

4.1 Optimization of input power using monitored signal

In achieving optimal XPM wavelength conversion, input power is an important tuning parameter. This is because $\Delta\phi$ (the amount of phase change in SOA_{mod}) should be kept at π for optimal XPM operation, and it is determined by the input power ratio of the two lights (signal and CW). In this section, in order to detect and keep the state of optimal XPM operation, we focus on the amplified signal (see Fig. 1) at SOA_{mod}. The wavelength of the amplified signal is the same as the input signal.

Figure 8(a) shows the schematic of the converted output signal power $P_{c\text{-}out}$ as a function of the input signal power $P_{s\text{-}in}$. With increasing $P_{s\text{-}in}$, $P_{c\text{-}out}$ changed from the maximum to the minimum value. The amount of $P_{c\text{-}out}$ change is defined as the extinction ratio (ER). The input signal power where ER is maximum is defined as $P_{s\text{-}in\text{-}conv}$. Fig. 8(b) shows the change in $P_{c\text{-}out\text{-}XGM}$. This is the converted output signal power when I_{pc} = 0 mA. In other words, it is the output power converted by cross-gain modulation (XGM). The $P_{c\text{-}out\text{-}XGM}$ reduction when the input signal power increases to $P_{s\text{-}in\text{-}conv}$ is equal to the gain change ΔGc (dB) in SOA_{mod}. Here, ΔGc should be

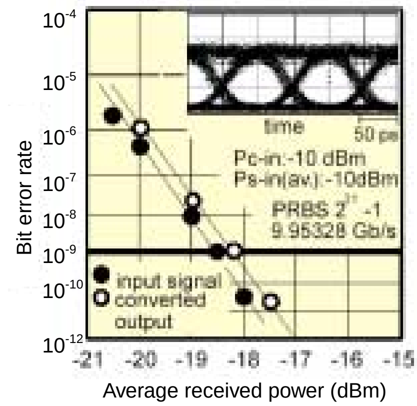

Fig. 6. 10-Gbit/s bit error characteristics and output eye pattern.

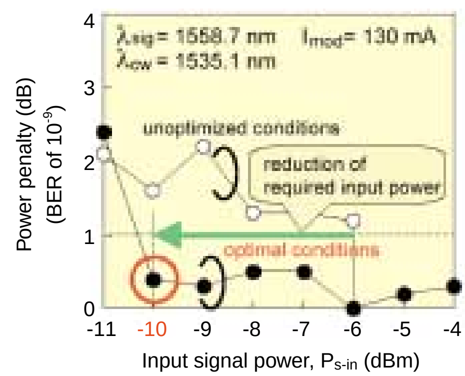

Fig. 7. 10-Gbit/s low input power operation.

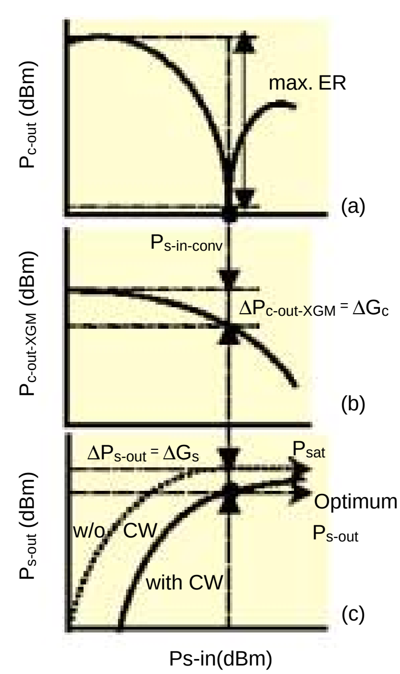

Fig. 8. Output power of (a) converted output signal $P_{c\text{-}out}$ (XPM), (b) converted output signal $P_{c\text{-}out\text{-}XGM}$ (XGM, Ipc =0 mA), (c) amplified signal $P_{s\text{-}out}$.

constant in order to keep optimal phase change $\Delta\phi = \pi$. Figure 8(c) shows the change in amplified signal power $P_{s\text{-}out}$. The dotted line shows the curve before input of CW light (w/o CW) and the solid line shows the curve after input of CW light (with CW). When the input signal power reaches $P_{s\text{-}in\text{-}conv}$, $P_{s\text{-}out}$ (w/o CW) reaches the saturated output power P_{sat}. When the CW light is input, the total gain is distributed between the two lights (signal and CW). Therefore $P_{s\text{-}out}$ (with CW) no longer reaches P_{sat} when the input signal power reaches $P_{s\text{-}in\text{-}conv}$. $P_{s\text{-}out}$ (with CW) is reduced by a definite value from P_{sat} (= $\Delta P_{s\text{-}out}$). These relationships are summarized as:

$$P_{c\text{-}out\text{-}XGM} + P_{s\text{-}out}\,(\text{with CW}) = P_{sat}\,(\text{mW: constant})$$

This equation shows that the total output power is always constant in the saturation region. Therefore, when the optimal gain change ΔGc (= $\Delta P_{c\text{-}out\text{-}XGM}$) occurs in SOA_{mod}, $\Delta P_{s\text{-}out}$ (with CW) also becomes constant. In an experiment, we only need to measure the average output power of $P_{s\text{-}out}$ (with CW) and keep it constant. Then the optimal condition will be maintained. As an example of the optimal value of $P_{s\text{-}out}$ (with CW), if ΔGc = 3dB, it will be 3 dB below P_{sat}. Hereafter, we call the average output power of $P_{s\text{-}out}$ (with CW) the monitor signal power.

4.2 Variable XPM-WC

In this section, we discuss the variable wavelength conversion of an XPM-WC using the input power tuning technique described above. When we change the output wavelength from λ_1 to λ_2 smoothly, it is necessary to optimize the input power of the CW light while changing its wavelength. At this time, we only need to measure and keep the monitor signal power instead of observing the eye pattern of the converted output signal. The CW light power is optimized so that the monitor signal power may keep the optimal value. Figure 9 shows the experimental setup for the variable wavelength conversion of the XPM-WC. The CW source is a super-structure grating (SSG) DBR laser. We employed 30 wavelengths (λ_1-λ_{30}) from 1539.8 nm with a channel spacing of 100 GHz. The wavelength of the input signal was set to λ_{16}. The input signal was modulated at 10 Gbit/s (NRZ format, PRBS 2^{31}-1), and the average input power was set to -8 dBm. The monitor signal power was measured at the output of the arrayed waveguide grating (AWG) filter. The input CW light power was optimized so that the monitor signal power would hold. We measured the BER characteristics and the converted output signal power for every wavelength change.

Figure 10 shows the results of wavelength change operation. The horizontal axis shows the optical channel number. The left axis of Fig. 10(a) shows input CW light power $P_{c\text{-}in}$ and the right axis shows monitor signal power $P_{s\text{-}out}$. The white circles show the uncontrolled $P_{c\text{-}in}$ (outputs of the SSG-DBR-LD). The gray circles show the optimized $P_{c\text{-}in}$. They were adjusted so that the monitor signal power (black diamonds) might be fixed at -5.2 dBm. In Fig. 10(b), the left axis shows the converted output signal power $P_{c\text{-}out}$ and the right axis shows the excess power penalty in the back-to-back condition. Among the 30 channels (wavelength range of 24 nm), the Pc-out change was less than 1 dB (-3.6 to -4.6 dBm) and the power

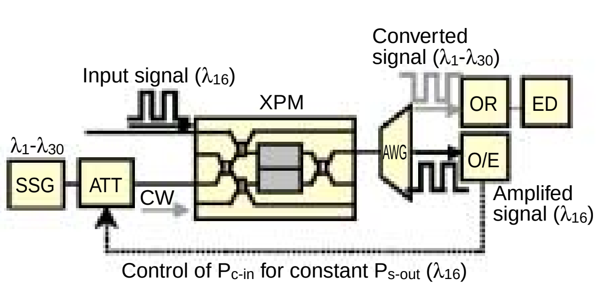

Fig. 9. Experimental setup for variable XPM wavelength conversion.

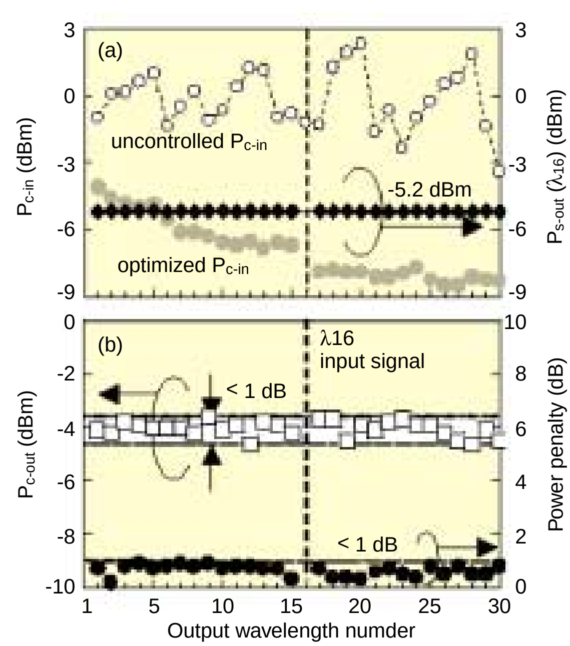

Fig. 10. Results of variable wavelength conversion. (a) Left axis: uncontrolled and optimized input CW power and Right axis: monitor signal power. (b) Left axis: converted output signal power Right axis: back-to-back power penalty.

Fig.11. Variable XPM-WC unit.

penalty was less than 1 dB. These results show the effectiveness of the proposed optimal tuning technique using a monitor signal.

We fabricated a variable XPM-WC unit (Fig. 11). It consists of XPM-WCs, a variable CW source (SSG-DBR-LD), and a CW level controller. They operate simultaneously using a common controller. By employing the above tuning technique, we can easily set the optimal input CW power to each selected wavelength. The CW level controller is an auto gain loop control circuit using an SOA [15]. Other tuning parameters, such as I_{mod} and I_{pc}, and module temperature are set in advance in the common controller. According to the chosen output wavelength, all optimal tuning parameters are set automatically, and stable wavelength conversion is carried out. The wavelength switching time of this unit was estimated to be less than 5 ms, which is sufficiently fast for wavelength path routing [16].

5. Conclusion

We examined practical issues in XPM-WCs, especially low-power operation and optimal tuning. From the relationship between I_{pc} and the eye opening ratio, we clarified the optimal current condition for low-power operation. As a result, we achieved -10 dBm input power operation at a low total current. To maintain the optimal XPM operation, we found a condition where the monitor signal power should be constant. Using this principle, we successfully achieved variable wavelength conversion among 30 wavelengths. To improve the functionality of the wavelength converter and make it easier to use, we developed an XPM-WC unit that operates with a variable CW light source simultaneously and automatically.

References

[1] K. Sato, S. Okamoto, and H. Hadama, “Network performance and integrity enhancement with optical path layer technologies,” J. Select. Areas Commun., Vol. 12, pp. 159-170, January 1994.

[2] R. Sato, T. Ito, K. Magari, A. Okada, M. Oguma, Y. Suzaki, Y. Kawaguchi, Y. Suzuki, A. Himeno and N. Ishihara, “Polarization insensitive SOA-PLC hybrid integrated Michelson interferometric wavelength converter and its application to DWDM networks,” IEICE Trans. Electron., Vol. E84-C, pp. 571-578, 2001.

[3] C. Janz, B. Dagens, A. Bisson, F. Poingt, F. Pommereau, F. Gaborit, I. Guillemot, and M. Renaud, “Integrated all-active Mach-Zehnder wavelength converter with record signal sensitivity and large dynamic range at 10Gb/s,” Optical Fiber Communication ’99, San Diego, U.S.A., FB3, pp. 30-32, Feb. 1999.

[4] L. H. Spiekman, U. Koren, M. D. Chien, B.I. Miller, J.M. Wiesenfeld, and J. S. Perino, “All optical Mach-Zehnder wavelength converter with monolithically integrated DFB probe source,” IEEE Photon. Technol. Lett., Vol. 9, pp. 1349-1351, 1997.

[5] T. Durhuus, B. Mikkelsen, C. Joergensen, S. L. Danielsen, and K. E. Stubkjaer, “All-optical wavelength conversion by semiconductor optical amplifiers,” J. Lightwave Technol., Vol. 14, pp. 942-954, 1996.

[6] D. Wolfson, A. Kloch, T. Fjelde, C. Janz, B. Dagens, and M. Renaud, “40-Gb/s all-optical wavelength conversion, regeneration, and demultiplexing in an SOA-based all-active Mach-Zehnder interferometer,” IEEE Photon. Technol. Lett., Vol. 12, pp. 332-334, 2000.

[7] B. Mikkelsen, S. L. Danielsen, C. Joergensen, R. J. S. Pedersen, H. L. Poulsen, and K. E. Stubkjaer, “All-optical noise reduction capability of interferometric wavelength converter,” Electron. Lett., Vol. 32, pp. 566-567, 1996.

[8] Y. Nakasuga, T. Hashimoto, Y. Yamada, M. Yanagisawa, K. Moriwaki, Y. Akahori, Y. Tohmori, K. Kato, S. Sekine, and M. Horiguchi, “Multi-chip hybrid integration on PLC platform using passive alignment technique,” Electronic Components and Technology Conference ’96, Orlando, U.S.A., pp. 20-25, May 1996.

[9] N. Uchida, Y. Hibino, Y. Suzuki, T. Kurosaki, N. Ishihara, M. Nakamara, T. Hashimoto, Y. Akahori, Y. Inoue, K. Moriwaki, Y. Yamada, K.

Kato, Y. Tohmori, M. Wada, and T. Sugie, "Passively aligned hybrid WDM module integrated with a spot-size converted laser diode and waveguide photodiode on a PLC platform for fiber-to-the-home," Optical Fiber Communication '96, San Jose, U.S.A., PD-15, March 1996.
[10] T. Ito, I. Ogawa, Y. Suzaki, K. Magari, and Y. Kawaguchi, "Simultaneous 4-channel wavelength conversion using four-wave mixing in an PLC-SOA hybrid wavelength selector," Optical amplifiers and their applications (OAA), FB2, Nara, Japan, 1996.
[11] T. Kawai, M. Teshima H. Yasaka, H. Takahashi, and M. Koga, "Optoelectronic wavelength conversion scheme using DFB-LDs and optical switch for VWP photonic transport system," Optoelectronics and Communications Conference'98, Chiba, Japan, 13A2-3, pp. 22-23, July 1998.
[12] R. Sato T. Ito, K. Magari, Y. Inoue, I. Ogawa, R. Kasahara, M. Okamoto, Y. Tohmori, Y. Suzuki and N. Ishihara, "Low input power (–10 dBm) SOA-PLC hybrid integrated wavelength converter and its 8-slot equipment," European Conference on Optical Communication '01, Amsterdam, Holland, Th.F.2.3, Sep. 2001.
[13] R. Sato T. Ito, K. Magari, J. Endo, I. Ogawa, Y. Inoue, R. Kasahara, Y. Tohmori, and Y. Suzuki, "Novel tuning technique to optimize input power of a variable wavelength converter using cross-phase modulation (XPM)," Proc. Photonics in Switching'02, Cheju Island, Korea, MoB3, July 2002.
[14] N. Yoshimoto, K. Magari, Y. Kawaguchi, K. Kishi, Y. Kondo, Y. Kadota, T. Ito, O. Mitomi, Y. Tohmori, Y. Yoshikuni, O. Nakajima, and Y. Hasumi, "Four-channel polarization-insensitive SOA gate array integrated with butt-joined spot-size converters," Electron. Lett., Vol. 33, pp. 2045-2046, 1997.
[15] J. Endo, A. Ohki, R. Sato, T. Ito, Y. Tohmori, and Y. Suzuki, "Wide input dynamic range cross-phase modulated wavelength conversion using an SOA-based automatic power equalizer," OECC'02, Yokohama, Japan, 12C3-1 July 2002.
[16] N. Agrawal, E. S. Tentarelli, N. A. Jackman, L. Zhang, S. S. K. Korotky, B. H. Lee, S. Baroni, B. B. M. Comissiong, J. M. Hitchcock, Y. R. Bing, J. P. Hickey, A. M. Gottlieb, K. S. Bhalla, T. W. Van Blarcum, D. T. Neilson, C. R. Giles, V. A. Aksyuk, S. Arney, N. R. Basavanhally, D. J. Bishop, B. A. Boie, C. A. Bolle, J. V. Gates, P. R. Kolodner, F. Pardo, R. Ruel, and R. E. Scotti, "Demonstration of distributed mesh restoration and auto-provisioning in a WDM network using a large optical cross-connect," Optical Fiber Communication'00, Baltimore, U.S.A., Vol. 4, PD-37, pp. 278-280, March 2000.

Rieko Sato
Research Engineer, Photonics Integration Project, NTT Photonics Laboratories.
She received the B.E. and M.E. degrees from Tsukuba University, Ibaraki, Japan in 1992 and 1994, respectively. In 1994, She joined NTT Opto-electronics Laboratories (now Photonics Laboratories). She is engaged in research and development on hybrid integrated optical modules based on semiconductor optical amplifiers. Ms. Sato is a member of the Institute of Electronics, Information, and Communication Engineers (IEICE) of Japan and IEEE Lasers and Electro-optics Society.

Toshio Ito
Senior Research Engineer, Photonics Integration Project, NTT Photonics Laboratories.
He received the B.S. and M.E. degrees from Keio University, Kanagawa, Japan, in 1986 and 1988, respectively. In 1988, he joined the Musashino Electrical Communications Laboratories, where he engaged in research on parallel processing systems and communication switching systems. Since 1993, he has been engaged in research on the InGaAlAs/InAlAs multi-quantum well optical switches, InGaAsP semiconductor optical amplifiers, and wavelength converters at NTT Photonics Laboratories, Kanagawa, Japan. Mr. Ito is a member of the IEICE, JSAP, and OSA.

Ikuo Ogawa
Senior Research Engineer, Photonics Integration Project, NTT Photonics Laboratories.
He received the B.S. and M.S. degrees in applied physics from Waseda University, Tokyo, Japan, in 1990 and 1992, respectively. In 1992, he joined the NTT Opto-electronics Laboratories. Since then he has been engaged in research and development on silica-based planar lightwave circuits and hybrid integrated optical devices. He now works at the NTT Photonics Laboratories. Mr. Ogawa is a member of the Institute of Electronics, Information and Communication Engineers (IEICE) of Japan, and the IEEE Lasers and Electro-optics Society.

Hiroshi Okamoto
Senior Research Engineer, Photonic Device Laboratory, NTT Photonics Laboratories.
He received the B.E., M.E. and Dr. E. degrees from Chiba University, in 1981, 1983, and 1998, respectively. In 1983, he joined NTT Electrical Communications Laboratories. Since then, he has been engaged in the MOVPE growth, semiconductor-crystal characterization, and research and development on semiconductor devices. He is now a Senior Research Engineer in the Photonic Device Laboratory in NTT Photonics Laboratories. Dr. Okamoto is a member of the IEEE Laser and Electro-Optics Society (LEOS), the IEEE Components, Packaging, and Manufacturing Technology Society (CPMT), the IEEE Electron Devices Society (ED), the Institute of Electronics, Information and Communication Engineers (IEICE) of Japan, and the Japan Society of Applied Physics (JSAP).